JOURNAL OF MATERIALS SCIENCE 20 (1985) 4532–4552

Effect of isothermal exposure on fatigue crack growth in boron–titanium composites

J. M. QUENISSET, P. SOUMELIDIS, R. PAILLER, R. NASLAIN
Laboratoire de Chimie du Solide du CNRS, Université de Bordeaux, 351 Cours de La Libération, 33405 Talence Cedex, France

N. S. STOLOFF
Materials Research Center, Rensselaer Polytechnique Institute, Troy, New York 12181, USA

Fatigue crack growth testing has been applied to boron/Ti–6Al–4V composites in order to investigate simultaneously crack propagation mechanisms during the fatigue and overload portion of the experiments. It is concluded that linear elastic fracture mechanics (LEFM) for heterogeneous and anisotropic materials facilitates understanding of the rupture mechanisms and the assessment of failure work and toughness. The influence of isothermal exposure on crack propagation mechanisms has been pointed out. A short duration heat treatment at 850° C improves the composite toughness and reduces the fatigue crack growth rate although the fibre–matrix (FM) interfacial bonding is increased. This effect has been related to a damage mechanism initiated in the interfacial reaction zone. In any case, the fatigue behaviour of the composite is controlled by the matrix and the capability of the fibres to function as crack arrestors. The impeding effect of the fibres is no longer effective when the thermal exposure duration is significant.

1. Introduction

Most synthetic metal matrix composites (MMC) such as boron/Ti–6Al–4V are expected to be used at high temperature since a metal matrix has higher thermal stability than an organic matrix [1, 2]. However, they are non-equilibrium systems from a thermodynamic stand point and solid state reactions occurring by diffusion at the FM interfaces restrict their usefulness. Such chemical reactions must be carefully controlled during processing and use, in order to ensure sufficient adhesion for load transfer and to avoid the excessive growth of a brittle layer between fibre and matrix that will result in loss of strength. The importance of FM interface behaviour on MMC tensile strength has been pointed out previously by several authors through theoretical and experimental studies [3–13]. Moreover, transverse strength, mechanical and thermal fatigue behaviour, impact behaviour and fracture toughness studies have also demonstrated the influence of FM interfaces on mechanical properties [14–26].

Nevertheless, very little work has been done to apply fatigue crack growth to investigate simultaneously fracture mechanics, fatigue properties and toughness of composites, particularly with respect to interface behaviour. While LEFM has been very helpful in describing crack propagation in metals, the use of LEFM concepts for composites has led to considerable difficulties such as:

1. determining a stress intensity factor in orthotropic and heterogeneous materials for which the crack tip stress distributions depend on the materials properties and orientations;

0022–2461/85 $03.00 + .12

2. considering one of the crack failure modes (I, II or III) despite the fact that the application of a single load mode leads, in general, to crack tip displacements of mixed mode (e.g. opening mode I and sliding mode II);

3. using a compliance calibration technique which is often unreproducible and not valid for orthotropic heterogeneous materials [27–31].

The first objective of this study was to determine whether fatigue crack growth testing of synthetic MMC could provide a suitable method for understanding fracture behaviour related to interface features. The usual fatigue crack growth techniques using optical observation of the crack or electrical gauges have been combined with metallography and scanning electron microscopy techniques in order to assess the significance of the results and to correlate mechanical behaviour and interface features. Emphasis has been placed on the effect of isothermal exposures on crack propagation behaviour and toughness of unidirectional boron/Ti–6Al–4V composites for which FM reaction is rather important and well known [32].

The second aim of this study was to establish whether mechanical properties of the synthetic MMC could be adjusted by diffusion heat treatments.

2. Fatigue crack propagation

Fatigue crack propagation is an interesting method for investigating MMC mechanical behaviour because:

1. many small cracks exist in as-fabricated synthetic MMC due to mechanical or thermal degradation during processing, particularly at the FM interfaces. Therefore, the incubation time of the fatigue failure mechanism is restricted to the time during which an existing crack fails to grow so that fatigue crack propagation becomes of major importance.

2. control of the crack growth rate allows examination of the fracture mechanisms with respect to the local stress level (stress intensity factor) when the material is initially fatigued and then overloaded. Therefore, fatigue crack growth provides a better understanding of the interaction between cracks and fibres.

3. finally, comparisons between composites can be approached through fracture toughness and, therefore, rupture work.

Thus, several mechanical characteristics of the material can be simultaneously assessed which permits one to point out the influence of different parameters (processing conditions, heat treatment, testing conditions) on the material behaviour with a smaller number of specimens.

3. Materials

3.1. Unidirectional Ti–6Al–4V/boron composites

Unidirectional boron/Ti–6Al–4V composites were chosen for this study on the basis of the following considerations:

1. chemical vapour deposition (CVD) ceramic filament–titanium composites are potential materials for applications at medium temperatures (up to about 500° C);

2. the melting point of titanium is high enough (i.e. 1668° C) to allow diffusion treatments over a wide temperature range;

3. chemical reaction at the interfaces between boron fibres and titanium alloys is sufficiently rapid to result in a marked effect of heat treatment on mechanical behaviour;

4. the FM reaction zone, corresponding to a well known phase diagram (Ti–B), has been extensively studied, allowing correlations between the interface layer features and mechanical test results [5, 7, 10, 32].

The specimens were prepared by hot pressing, under vacuum, thin Ti–6Al–4V foils (100 to 150 μm thick) and monolayers of aligned uncoated boron CVD filaments (140 μm diameter with a 12 μm tungsten core). The duration of hot pressing was 30 min at 850° C with a pressure of 90 MPa. The panels were then annealed for 45 min at 750° C under a pressure of 20 MPa. Details of the processing conditions have been given elsewhere [32].

The specimens were eight plies 80 mm × 80 mm × 2 mm plates with a fibre volume fraction, V_f, of about 32%. All the panels were prepared in the same way and cut by electro-discharged machining (EDM).

The mechanical characteristics of the materials, in the as-fabricated condition, have been measured from tension and bending tests or calculated according to the rule of mixtures [33]. The material has been considered quasi-isotropic in any direction perpendicular to the fibres (Table I).

TABLE I Mechanical characteristics of the boron/Ti–6Al–4V unidirectional composites (V_f = 32%)

		E_L* (GPa)	E_T* (GPa)	ν_L†	ν_T†	G_{LT}§ (GPa)	σ_L‡ (MPa)	σ_T‡ (MPa)
Ti–6Al–4V (annealed at 850° C)		108		0.33		40	1000	
Boron CVD fibre		400	–	0.2	–	170	3500	–
Experimental:	tensile	204	140	0.27	0.2	–	1000	340
	bending	173	150	–	–		1850	–
Calculated:	tensile	201	141	0.28	0.19	60	1630	286
	bending	194	143	–	–		1920	–

*E_L, E_T = longitudinal and transverse Young's modulus respectively.
†ν_L, ν_T = Poisson's ratio.
‡G_{LT} = shear modulus.
§σ_L, σ_T = rupture strength.

3.2. Diffusion heat treatments and FM reaction

Before testing, the specimens were sealed in evacuated silica tubes and diffusion heat treated at 850° C for 9, 18 or 36 h. After cooling, the specimens were notched for crack initiation as described below. The features of the interfacial zones and the amplitude of the chemical reaction were evaluated after fatigue crack growth by means of metallographic examination. The thickness of the brittle layer was found to be in good agreement with results previously reported [5, 7, 10, 32].

4. Experimental procedure

4.1. Testing

Fatigue crack growth testing was done in a tension–tension mode using a servo-hydraulic machine. All experiments were conducted in load control at a frequency of 20 Hz so that strain rate effects as well as time dependent effects (e.g. contribution of corrosion to crack growth) were avoided. The wave form was sinusoidal and the stress ratio was kept at R = 0.1 (minimum load/maximum load).

The specimens were pin gripped (6 mm diameter) and axially loaded with the help of homocinetic attachments.

4.2. Specimen shape

Attempts to use compact tension specimens led to crack growth along fibres due to the relatively poor transverse resistance of the composite with respect to longitudinal strength. Thus a single edge notched (SEN) specimen had to be designed. After several tests, the shape and dimensions defined in Fig. 1a were selected. Fibres were parallel to the longitudinal axis.

In order to avoid a long crack initiation time, a chevron notch was machined on each specimen as represented in Fig. 1b, by means of a thin diamond saw (0.4 mm thick). Under such conditions a small crack can be observed close to the tip of the machined notch, as soon as tension–tension load cycling is commenced.

4.2. Crack length measurement

Optical methods have been used to observe and measure the crack extension. A travelling cathetometer was combined with a stroboscope synchronized on the wave cycling frequency. The phase shift was adjusted in order to render the crack area visible only at the maximum load, i.e. when the crack was opened.

To check the validity of the optical crack length measurement, electrical gauges were attached to several specimens. The successive failures of the threads, corresponding to electrical

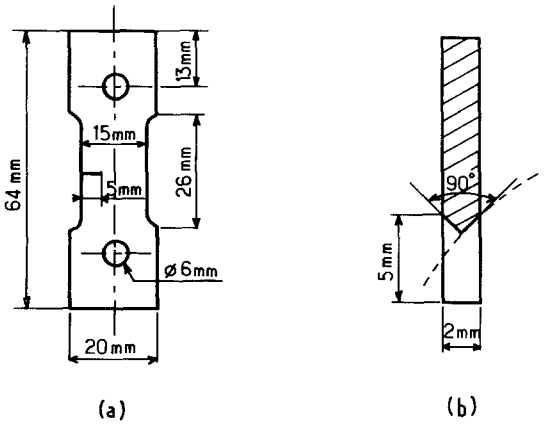

Figure 1 (a) Specimen shape and size. (b) Chevron notch.

resistance increases, allowed crack growth to be monitored. The measurements were not more accurate that those obtained when using the cathetometer, but a greater number of points could be recorded during the last steps of the crack propagation, i.e. when the crack growth rate was very high.

4.4. Computation of the numerical results

Regarding the expression which has to be chosen for the stress intensity factor K_I, the anisotropy and, above all, the heterogeneity of the composites have been the subject of many discussions [20, 34, 35]. The applicability of an expression corresponding to a homogeneous and isotropic material seems to be acceptable in the present case

$$\Delta K_I = YW^{1/2}(\sigma_{max} - \sigma_{min}) \quad (1)$$

with

$$Y = 1.99\left(\frac{a}{W}\right)^{1/2} - 0.41\left(\frac{a}{W}\right)^{3/2} + 18.7\left(\frac{a}{W}\right)^{5/2} - 38.48\left(\frac{a}{W}\right)^{7/2} + 53.85\left(\frac{a}{W}\right)^{9/2} \quad (2)$$

where W is the specimen width, a the crack length, σ_{max} and σ_{min} the maximum and minimum stress level.

Employing the previous approximation, the main crack growth parameters were evaluated according to three methods:

1. using the secant method, the crack growth rate da/dN against the stress intensity factor range ΔK_I could be plotted as illustrated in Fig. 2 [36]. From the quasi-linear part of the curve corresponding to a function $da/dN = C\Delta K_I^m$, m values as well as ΔK_I for $da/dN = 10^{-4}$ mm/cycle have been determined, and a first assessment of the critical stress intensity factor K_{Iac} has been obtained for the highest values of da/dN as shown in Figs. 2 and 3;

2. fitting the data with different equations of the crack length (a) against the number of cycles (N), it is possible to represent da/dN by an asymptotic function of ΔK_I similar to Forman's equation [37]

$$\frac{da}{dN} = \frac{C\Delta K_I^m}{(1 - R)K_{IC} - \Delta K_I} \quad (3)$$

with $R = \sigma_{min}/\sigma_{max}$, K_{IC} the fracture toughness, C and m material constants.

A reasonable fit of the data was obtained by the following equation as shown in Fig. 2

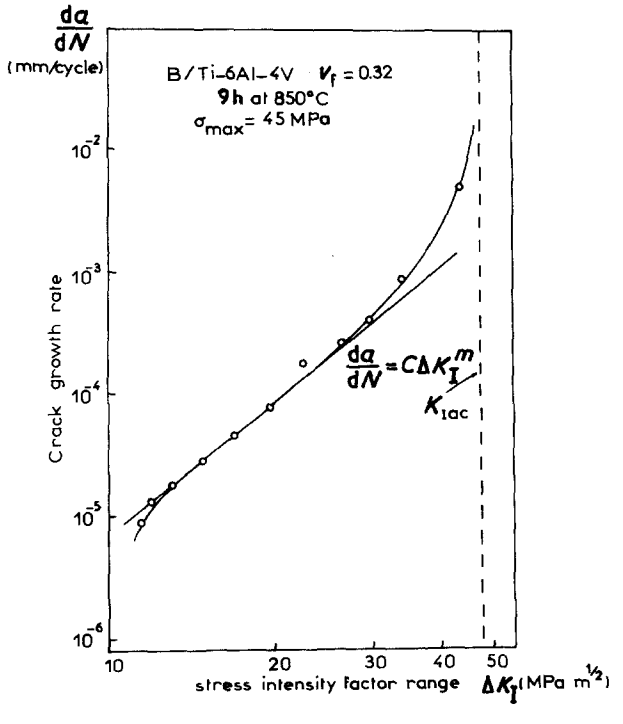

Figure 2 Crack growth rate plotted against stress intensity factor range derived from the secant method.

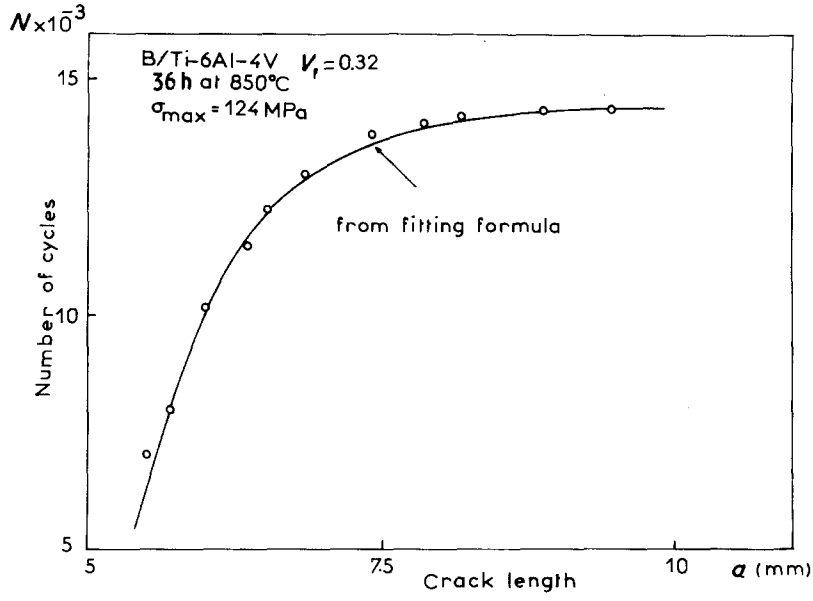

Figure 3 Crack length plotted against number of cycles.

$$N = A_1 + A_2 a^{[(2-m)/2]} + A_3 a^{[(3-m)/2]} \quad (4)$$

Computing Equations 1, 2 and 4 allowed us to plot da/dN against ΔK_I as illustrated in Fig. 4 and to derive K_{Iac}, m and ΔK_I for $da/dN = 10^{-4}$ mm/cycle;

3. determining the critical crack length a_c by a polynomial extrapolation of a plot of a–N for the number of cycles recorded at rupture, lead to calculation of K_{Iac} with Equation 1.

All the values obtained by the previous methods have been compared in order to assess the scatter shown in Figs. 7 to 9. The average values obtained for m, K_{Iac} and ΔK_I for $da/dN = 10^{-4}$ mm/cycle have been summarized in Table II.

5. Results and discussion

5.1. Failure mode

The observation of the crack profiles shows a crack opening mode very similar to that of metals. The crack growth is mainly coplanar with the notch, i.e. crack extension is perpendicular to the principal direction of elastic

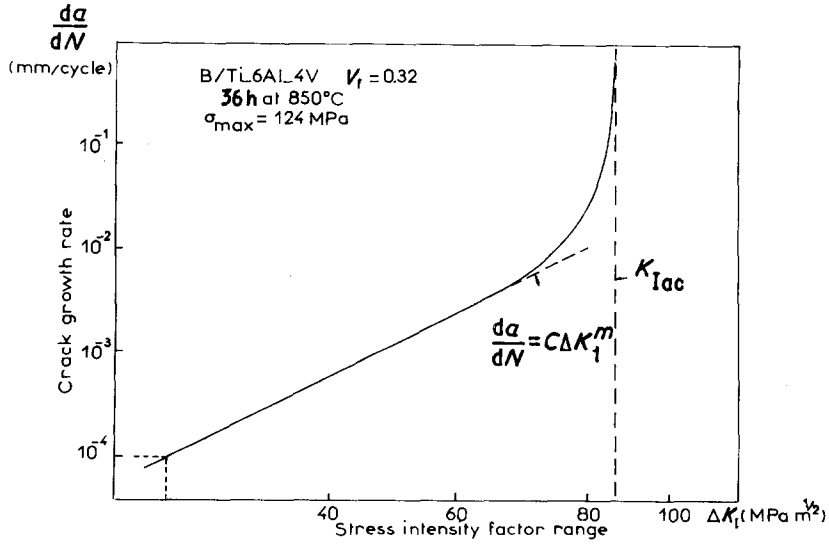

Figure 4 Crack growth rate plotted against stress intensity factor range derived from the fitting of Equation 4.

TABLE II Crack propagation parameters

Composite foil no.	σ_{max} (MPa)	Isothermal exposure at 850° C (h)	m	ΔK_I (MPa $m^{1/2}$) for da/dN = 10^{-4} mm/cycle	K_{Iac} (MPa $m^{1/2}$)
1	153	0	6	27	71
	122	9	3.4	25	86
	43	18	2.9	21	45
2	29	0	3.4	19	31
	36	9	2.6	20	50
3	58	0	3.3	20	48
	60	9	3	23	60
4	50	18	3	20	60
	50	36	4.2	21	58
5	90	0	3.6	23	60
	106	18	3.4	20	75
	108	36	4.6	23	74
6	124	0	4.5	25	75
	126	18	3.8	23	81
	124	36	4.8	24	83
7	44	9	3.5	20	47
8	133	0	3.8	26	75
	133	36	4.6	20	64

symmetry corresponding to the fibre orientation (Fig. 5). The predominance of the opening mode I and the regularity of the fatigue crack propagation curves lead us to consider the material as homogeneous for the macromechanical analysis of the quantitative results.

On the other hand, SEM microscopic examination reveals a stepped appearance of the

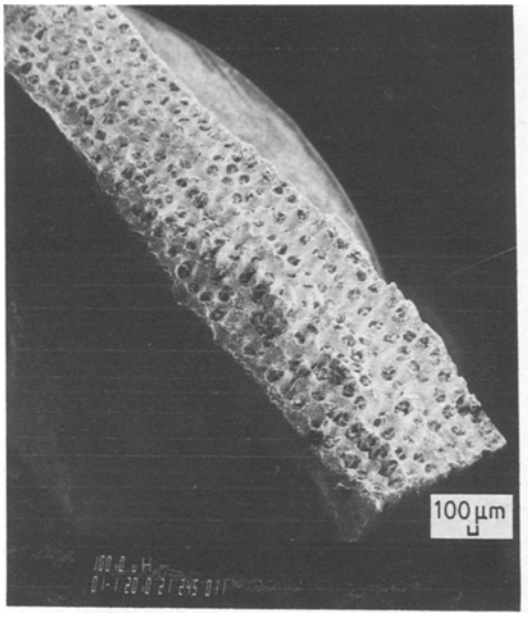

Figure 5 Scanning electron macrograph of fracture surface in B/Ti–6Al–4V composite after diffusion heat treatment (9 h, 850° C) and fatigue crack propagation.

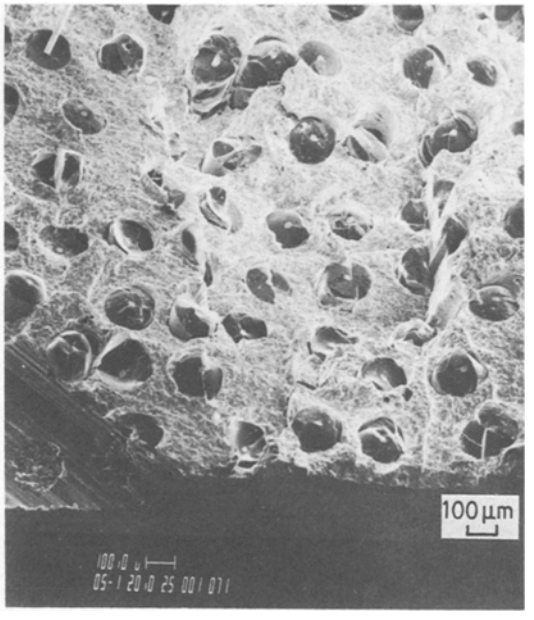

Figure 6 Scanning electron micrograph of fracture surface in B/Ti–6Al–4V heat treated composite (18 h, 850° C) showing intermittent excursion of fatigue crack along fibres.

fracture surface which is due to intermittent excursions of the crack along the fibre (Fig. 6). For microstructural and qualitative analysis of the failure, the composite has to be considered as heterogeneous with distinct components: fibres, interfacial zone and matrix.

5.2. Crack propagation characteristics

Assuming that the characteristics reported in Table II are representative (a point which will be discussed later) several general remarks can be made: (a) the crack growth rates are lower in the B/Ti–6Al–4V composites than in the corresponding annealed Ti–6Al–4V alloy. For $da/dN = 10^4$ mm/cycle most titanium alloys have $\Delta K_I \approx 11\,MPa\,m^{1/2}$; the average value obtained for B/Ti–6Al–4V composites is about $23\,MPa\,m^{1/2}$; (b) the slopes m of log (da/dN) – log ΔK_I curves are sometimes anomalously high and sometimes very low in comparison with titanium alloys ($2.5 < m < 6$ for B/Ti–6Al–4V composites; $m \approx 3.8$ for Ti–6Al–4V alloy); (c) the apparent critical stress intensity factor K_{Iac}, the exponent m and the fatigue crack growth rate (ΔK for $da/dN = 10^{-4}$ mm/cycle) exhibit a marked dependency on tensile stress level as illustrated in Figs. 7 to 9; (d) the fatigue threshold, below which no crack grows, could not be determined from the reported experiments. Indeed, measurement of the ΔK_I threshold requires the use of a low stress level which leads to a predominant mode II failure, as illustrated in Fig. 10. Since the crack extension is not coplanar with the notch, the previously described procedure for mechanical analysis cannot be applied. Thus the fatigue crack propagation mechanism for low stress level is difficult to represent quantitatively. Nevertheless, several experiments have shown that no mode I crack propagation occurs for $\Delta K_I < 10\,MPa\,m^{1/2}$.

5.3. Significance of the apparent critical stress intensity factors

To assess the significance of the apparent critical stress intensity factor with respect to toughness, the influence of numerous parameters should be studied. For instance, toughness should be independent of stress level, specimen configuration and thickness as well as testing conditions (cyclic frequency, wave form and stress ratio).

Since the aim of this study is not to generate data for design, these investigations have been limited to two questions: (a) what is the reason for K_{Iac} dependency on the stress level (Fig. 7), i.e. on the crack length? and (b) is the specimen thickness sufficient to provide plane strain conditions, i.e. is K_{Iac} unaffected by thickness?

5.3.1. K_{Iac} dependency on stress level

The K_{Iac} dependency on stress level can be attributed to several causes.

1. The compliance function in Equation 2 corresponds roughly to the specimen shape used in the present case. The exact function might differ slightly from Equation 2.

2. The compliance function should be modified to take into account the material anisotropy and heterogeneity.

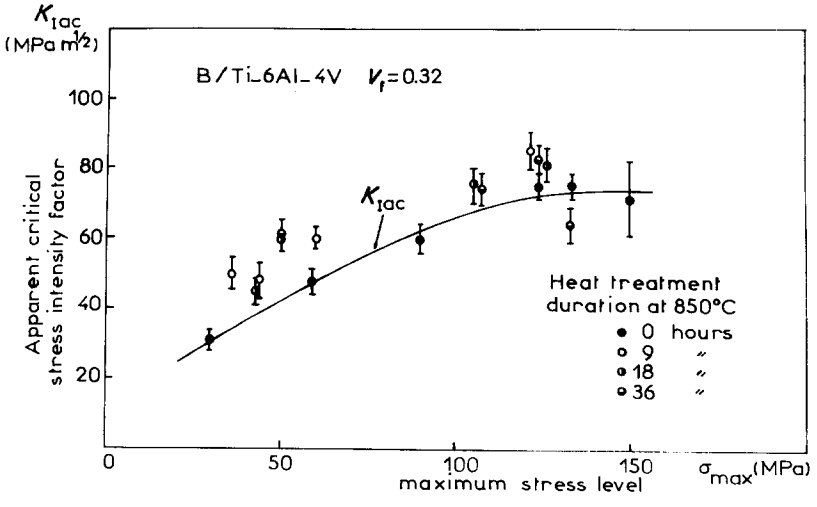

Figure 7 Influence of the maximum stress level on the apparent critical stress intensity factor.

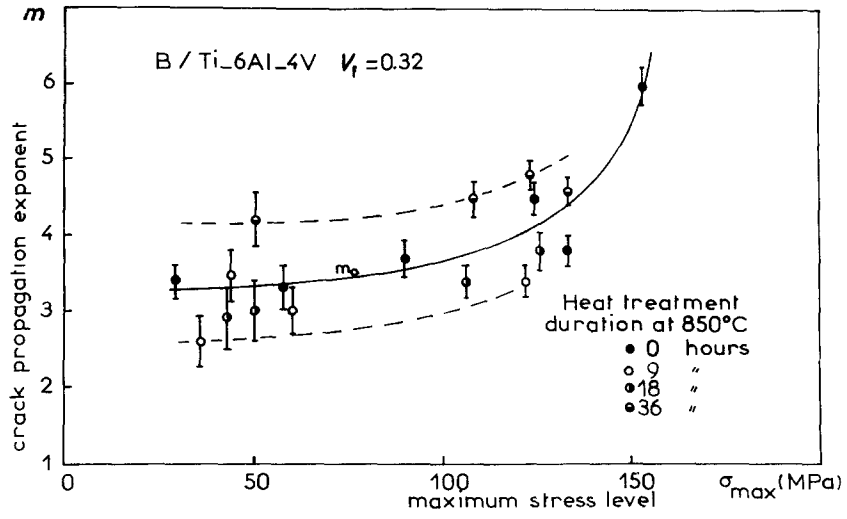

Figure 8 Influence of the maximum stress level on the crack propagation exponent.

3. Furthermore, for low stress levels, when the values of the critical crack lengths are more than half the distance between the tip of the notch and the specimen edge, the compliance function is no longer valid.

4. Otherwise, since the crack propagation mechanism is not the same for high and very low stress levels, an effect of the crack growth history might be expected: the same materials with a different crack growth history lead to different fracture characteristics.

This phenomenon could be related to the "crack skipping" effect following which unbroken fibre stringers retard the crack growth and therefore increase the material resistance to fracture [14]. However, this retardation effect should increase K_{Iac} while in the present case K_{Iac} decreases with crack length. Therefore, the crack skipping effect does not seem to be involved in the stress level dependency.

On the other hand, a reverse effect could lead to such a dependency. Because of the superior toughness of the matrix, ligaments of metal are expected to remain behind the primary crack front leading to a calculated ΔK_I smaller than the actual. This effect should be the more important as crack length increases, i.e. at low stress levels.

A degradation of the material by delamination along the FM interfaces, leading to crack blunting, could also be possible, particularly for

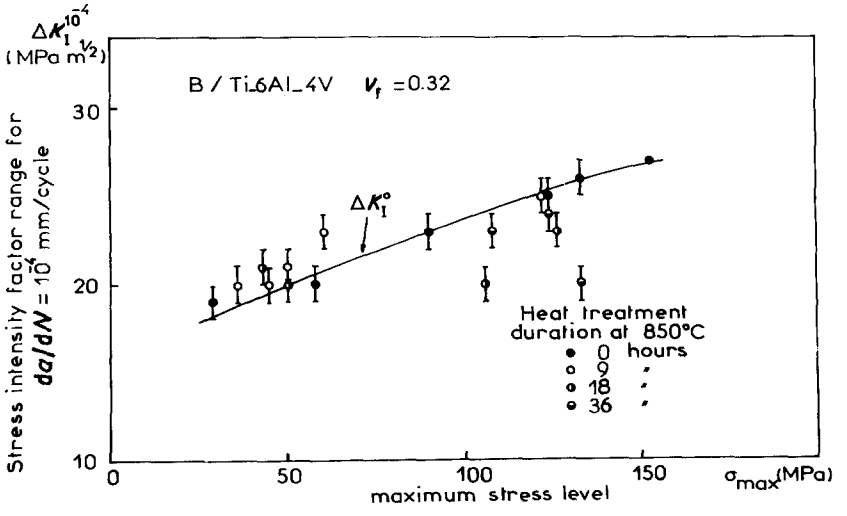

Figure 9 Influence of the maximum stress level on the crack growth rate.

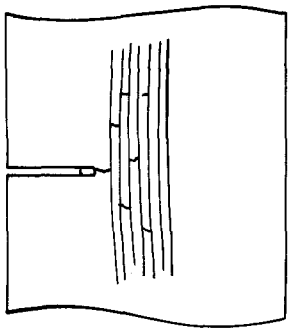

Figure 10 Schematic representation of fatigue crack growth for a low stress level.

low stress levels, i.e. for the longest fatigue life. However, no significant pull-out phenomenon has been observed.

Although no effect of the crack growth history remains presumable, the K_{Iac} dependency on stress level is negligible for high stress, as expected for short crack lengths, so that the corresponding K_{Iac} values will be considered for this study as the most representative of the material toughness values.

5.3.2. Thickness effect

The processing of homogeneous MMC by hot pressing parts over 2 mm thick is so difficult that the thickness effect on K_{Iac} could not be studied by using different specimen thicknesses. Thus, the thickness effect has been assessed by optical examination of the area located in the vicinity of the crack for each layer of the composites. The micrographs shown in Fig. 11 reveal a splitting zone on each side of the crack and points to considerable energy dissipation in a damage zone around the crack tip. This splitting phenomenon which concerns firstly the FM reaction zone, then the fibres, behaves as plastic deformation.

Therefore, the width, r_s, of the splitting zone has been used to check that yielding is confined to a small area ahead of the crack tip and to assess the material thickness which is in a state of plane strain. Fig. 12 shows a change in r_s close to the surface of the specimen but r_s remains constant in a thickness of about two-thirds of the overall specimen thickness. The observations have been confirmed by examination of the fracture surface exhibiting a 45° fracture plane only in the vicinity of the specimen surface and overloading zone, which is not the case after tensile rupture (Fig. 13).

Consequently, r_s appears to be nearly constant over the entire thickness of the specimen. This suggests that tri-axial stresses are high enough to consider that K_{Iac} provides a reasonable approximation of toughness with respect to the thickness effect.

On the other hand, r_s does not seem to be

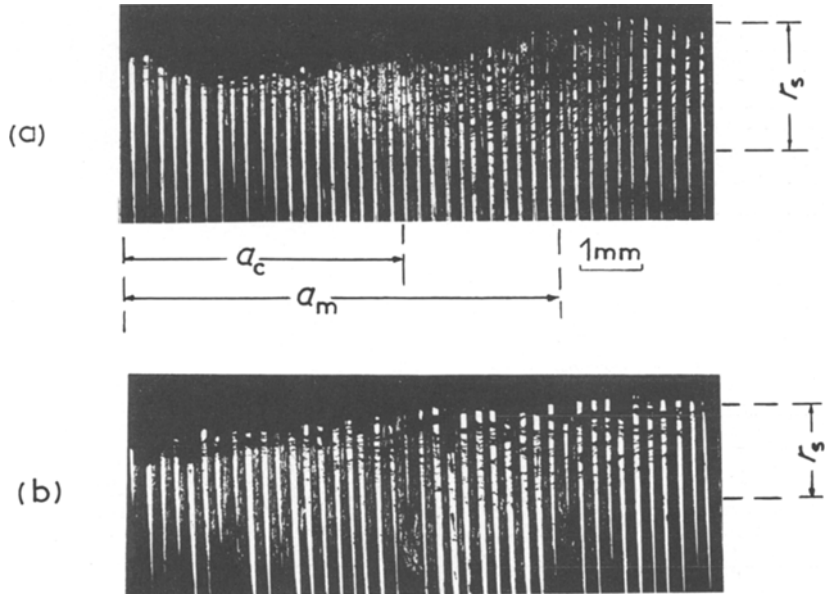

Figure 11 Micrograph of the splitting zone (isothermal exposure: 36 h, 850° C), (a) first boron filament layer, (b) fourth boron filament layer.

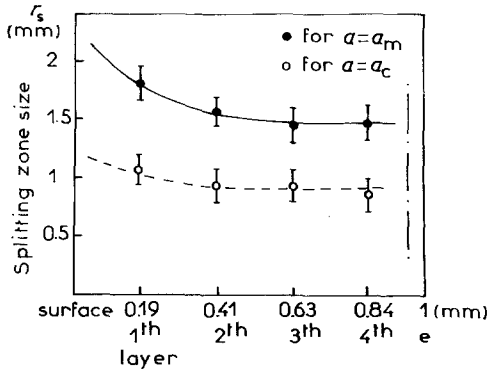

Figure 12 Width of the splitting zone as a function of the distance through the specimen thickness (isothermal exposure: 36 h, 850°C).

small enough, compared to the crack length a, to avoid a correction of K_{Iac} by using $(r_s + a)$ instead of a or by using a compliance calibration technique. However, when the plastic zone has a bulbous shape, as in the case of homogeneous isotropic materials, the splitting zone, corresponding to plastic deformation of the matrix, for an orthotropic material is more extended along the fibre direction and more constricted in the crack growth direction perpendicular to the fibres (Fig. 14). The effect is the stronger as the material is anisotropic and leads us to consider in the present case that r_s is only slightly smaller in the direction perpendicular to the fibres than along the fibres ($E_T/E_L = 0.7$).

However, no correction seems to be required to take account of the splitting zone in the crack length determination. Indeed, a strong discrepancy between the critical crack lengths a_c and the crack lengths a_m corresponding to the maximum width of the splitting zone increases the validity of the whole argument concerning the damage zone since $a_c < a_m$ (Fig. 11).

From the previous discussion about the significance of K_{Iac} as a toughness characteristic, K_{Iac} obtained for high stress level testing will be considered for further analysis and discussion as representative of the toughness of the boron/Ti–6Al–4V composites ($K_{IC} \approx 75\,MPa\,m^{1/2}$).

5.4. Effect of isothermal exposure

In order to emphasize the effect of isothermal exposure on the composite behaviour, the main characteristics of crack growth and rupture (K_{Iac}, m and ΔK_I for $da/dN = 10^{-4}$ mm/cycle) have been normalized with respect to the values corresponding to the as-fabricated composites and derived, for each stress level, from the fitting curves shown in Figs. 7, 8 and 9: K^0_{Iac}, m_0, ΔK^0_I for $da/dN = 10^{-4}$ mm/cycle.

The influence of diffusion heat treatments at 850° C during 9, 18 and 36 h, on these

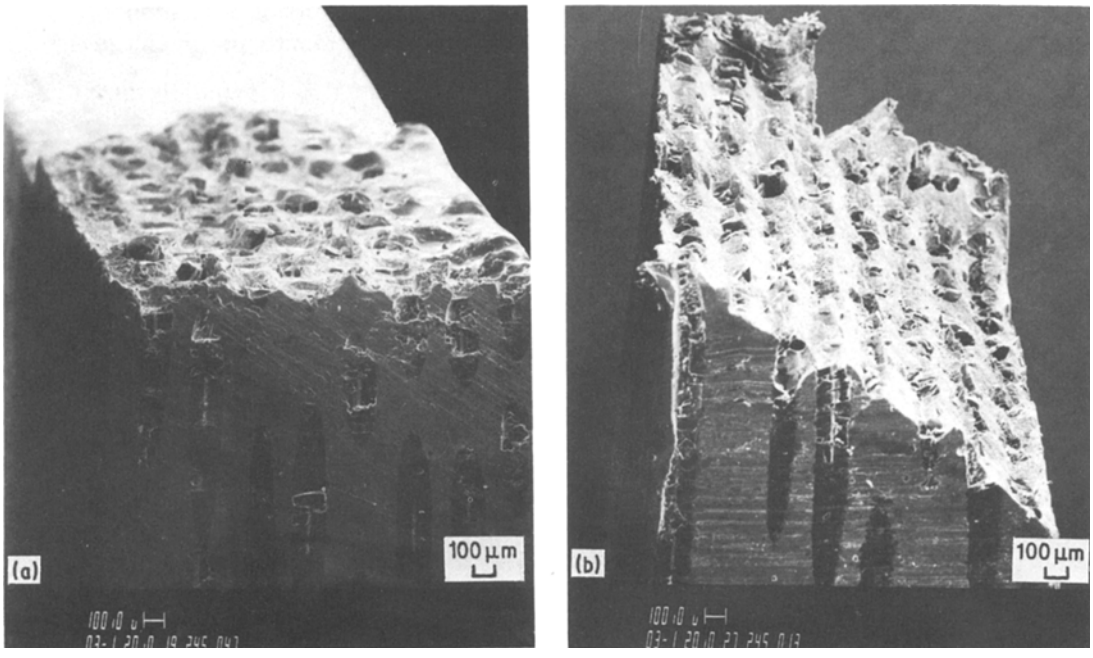

Figure 13 Macrographs of failure surfaces: (a) after crack propagation testing; (b) after tensile rupture.

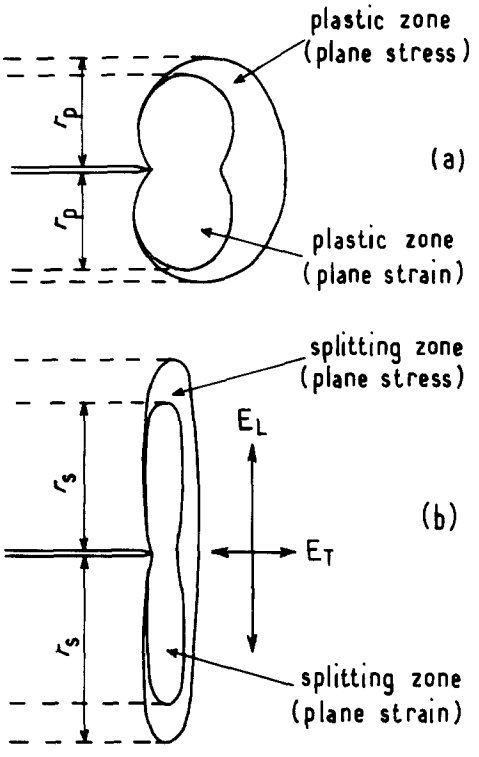

Figure 14 Damage zone shape and size for plane stress and plain strain conditions. (a) Isotropic material, (b) orthotropic material.

normalized characteristics and other parameters are shown in Figs. 15 to 19. Several observations can be summarized by the following remarks.

1. Heat treatment increases the matrix hardness by boron diffusion from fibres to matrix. The resulting increase in brittleness of the matrix should lead to a decrease in toughness of the matrix (Fig. 15).

2. The large extent of the splitting zone after relatively long heat treatments (18 h) is significant. Therefrom, the volume of matrix affected by plastic deformation, on each side of the crack, is increased by heat treatment. Thus and in spite of the matrix hardness increase, an increment of energy dissipation is expected after heat treatment (Fig. 16).

3. The crack propagation rate decreases for heat treatments up to 9 h and then increases slowly, showing a non-monotonic influence of the reaction zone thickness on crack growth (Fig. 17).

4. This evolution has to be compared with an inverse change in m when heat treatment time increases (Fig. 18).

5. The same evolution of the toughness with isothermal exposure time as for da/dN confirms the occurrence of a discontinuity in the composite behaviour with heat treatment (Fig. 19).

Thus, matrix hardness, FM interface bonding and the damage zone around the crack tip are increasing simultaneously with FM interfacial reaction zone thickness. The result is a non-monotonic change in crack growth parameters.

5.5. Fracture surfaces

Prior to any discussion about crack growth and rupture mechanisms, examination of fracture surfaces gives complementary indications:

1. The difference between the parts of the

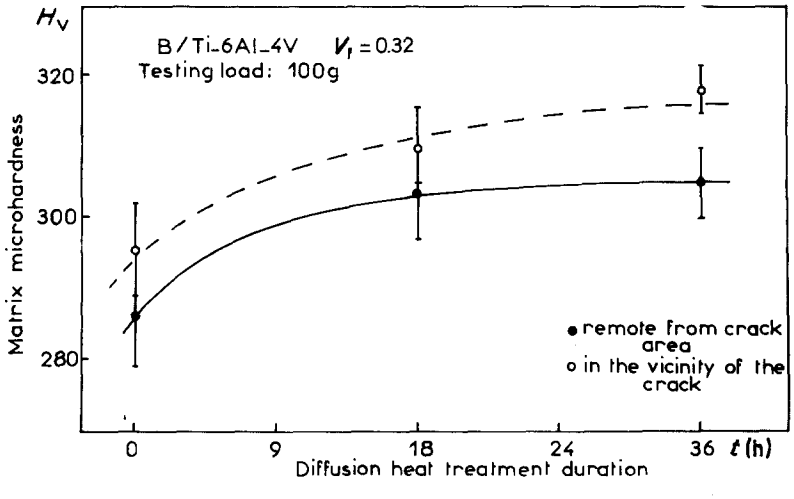

Figure 15 Effect of thermal exposure on matrix microhardness.

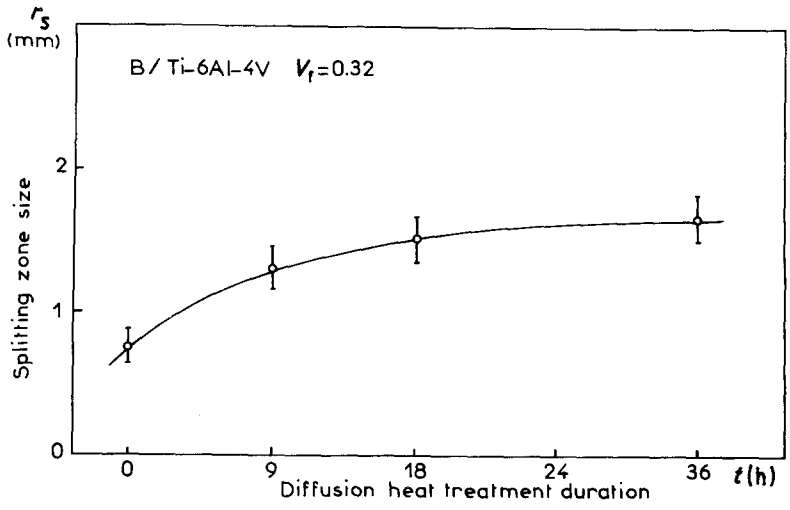

Figure 16 Effect of thermal exposure on the splitting zone size measured on the first boron filament layer of the specimen.

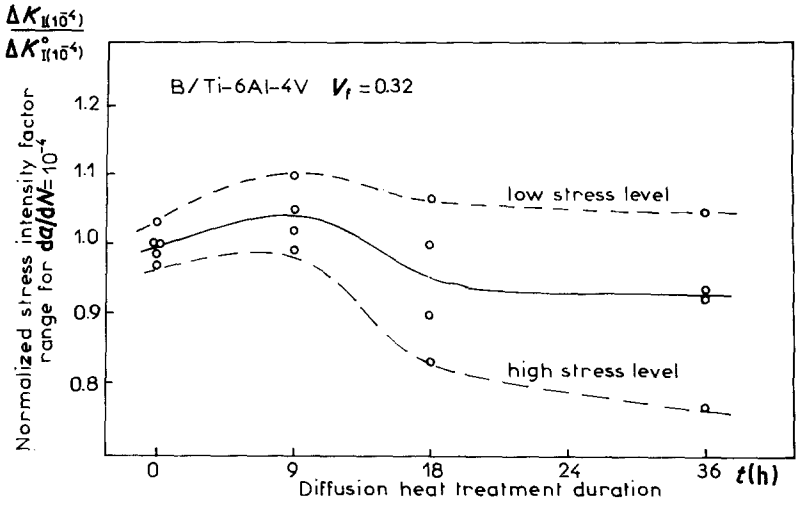

Figure 17 Effect of thermal exposure on crack growth rate.

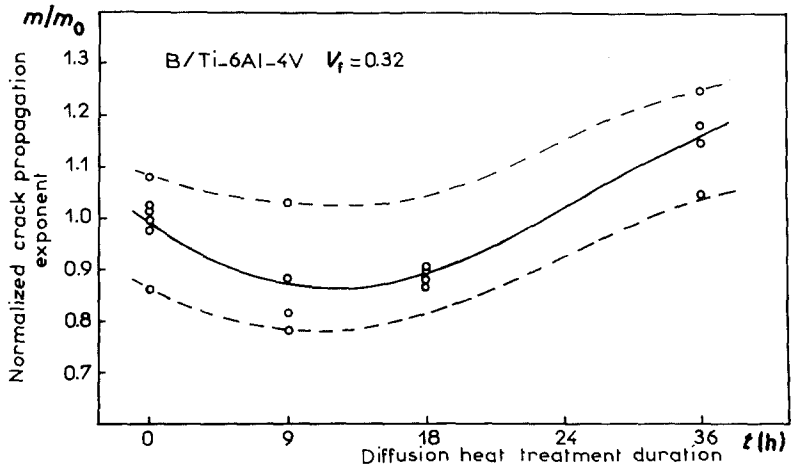

Figure 18 Effect of thermal exposure on crack propagation exponent.

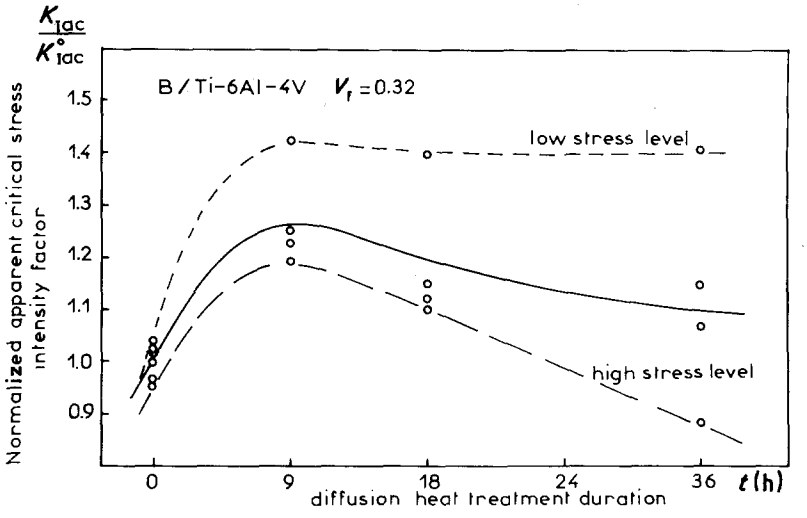

Figure 19 Effect of thermal exposure on toughness.

specimen which have failed by fatigue crack propagation and those corresponding to overloading is quite obvious (Fig. 20).

2. Although no pull-out phenomenon has been observed on fracture surfaces, a notable debonding effect can be seen for as-fabricated composites (Fig. 21).

3. When debonding occurs, the interfacial failure is situated between the reaction zone and the matrix for as-fabricated composites and between the reaction zone and the boron fibre when the composite is heat treated (Fig. 22).

4. Intermittent crack growth by mode II is enhanced by isothermal exposure (Fig. 23). Mode II cracks sometimes initiated in the locally hardened matrix when the crack approaches the reaction zone (Fig. 23a). They often follow longitudinal cracks in boron fibres (Fig. 23b), but they occur more commonly at fibre–reaction zone interfaces particularly after long diffusion heat treatments (Fig. 23c).

5. A long thermal exposure leads to significant tungsten core pull-out (Fig. 24a). This phenomenon associated with the Kirkendal effect

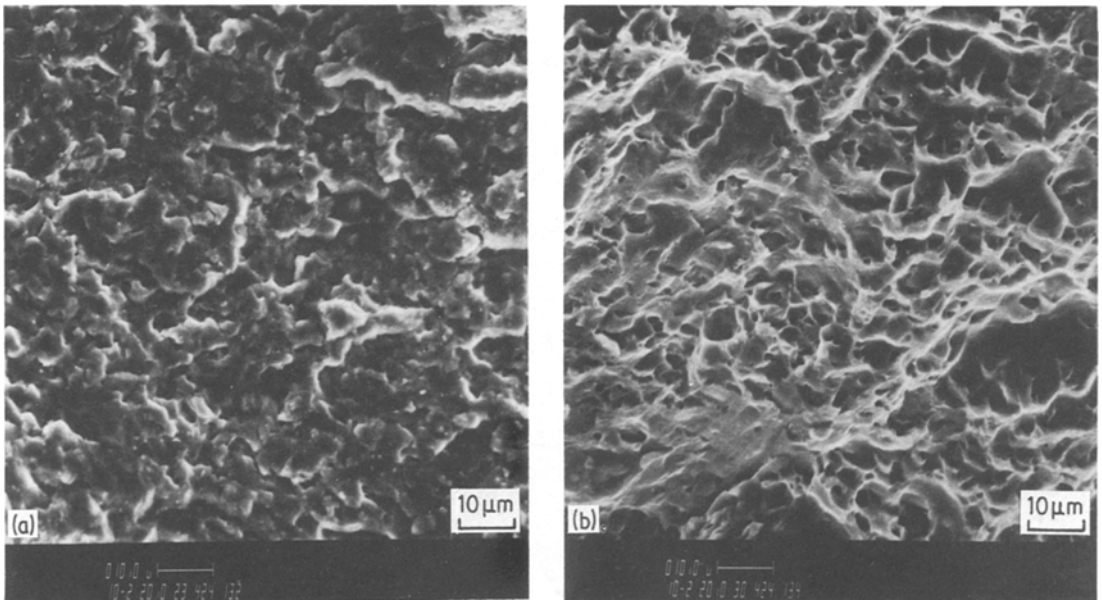

Figure 20 Scanning electron micrograhs of failure surfaces in Ti–6Al–4V matrix of as-fabricated B/Ti–6Al–4V composites: (a) fatigue zone, (b) overload zone.

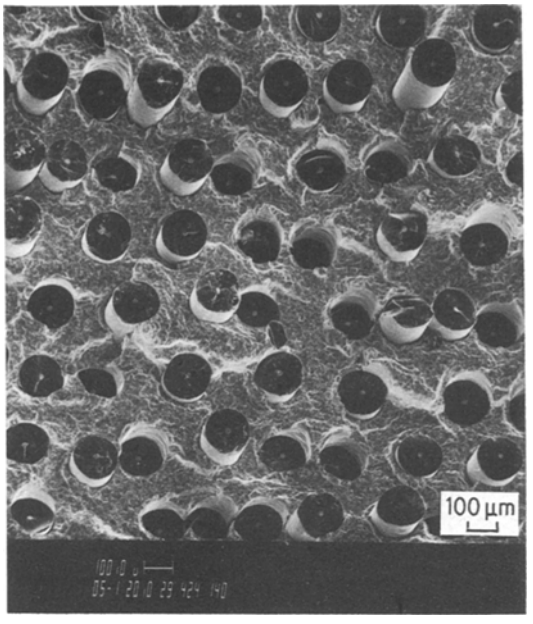

Figure 21 Scanning electron micrograph of failure surface in as-fabricated B/Ti–6Al–4V composite (fatigue zone).

due to boron diffusion from the fibres toward the matrix, suggests an extensive degradation of the reinforcement, as shown in Fig. 24b.

6. As soon as a reaction zone exists and is well bonded to the matrix by needle-like borides, numerous microcracks appear in the brittle phase, leading to crack initiation in the fibres and eventually propagation into the matrix (Fig. 25).

7. In as-fabricated composites, boron fibre fracture is most commonly initiated at the fibre core, as illustrated by the double cone fracture surface (Fig. 26).

In any case, fracture surfaces exhibit evidence of a retarding effect of the fibres (striations due to crack arrest by the fibres), slowing down the crack propagation rate.

5.6. Crack growth and rupture mechanisms

From the previously described results the crack propagation and rupture mechanisms can be schematically depicted as follows:

1. Fatigue crack propagation in B/Ti–6Al–4V composite materials is macroscopically very similar to fatigue crack growth in metals provided the maximum stress is not too low. Indeed, if the stress level is not high enough ($K_I < 10\,MPa\,m^{1/2}$), filaments function as crack arresters. Cracks are deflected along fibres and the composite material becomes notch insensitive, extending its fatigue life.

2. When the stress level is sufficiently high to induce transverse crack growth in a direction roughly perpendicular to the fibre axis, fibre

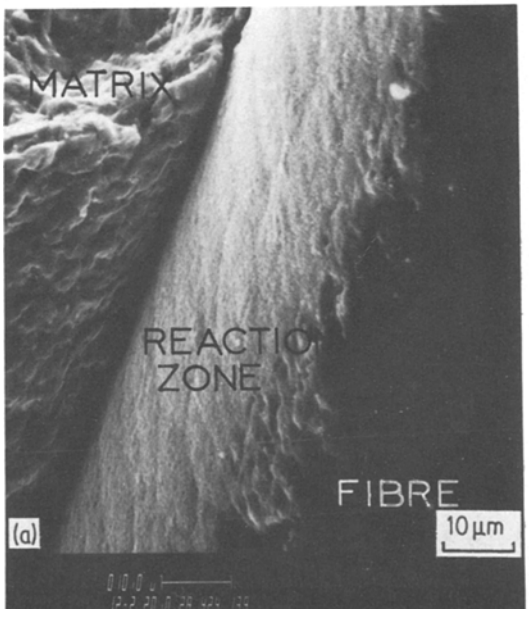

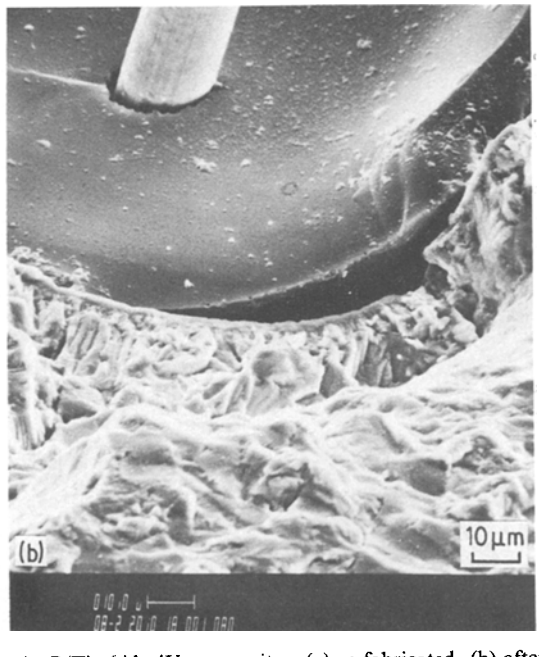

Figure 22 Scanning electron micrographs of interfacial failures in B/Ti–6Al–4V composites: (a) as-fabricated, (b) after isothermal exposure (36 h, 850°C).

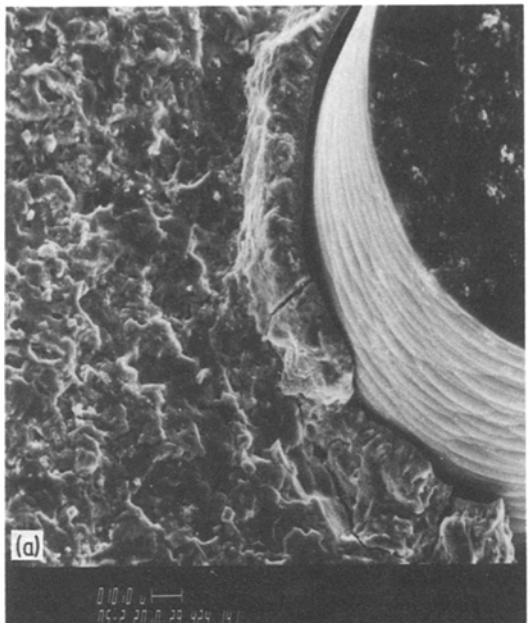

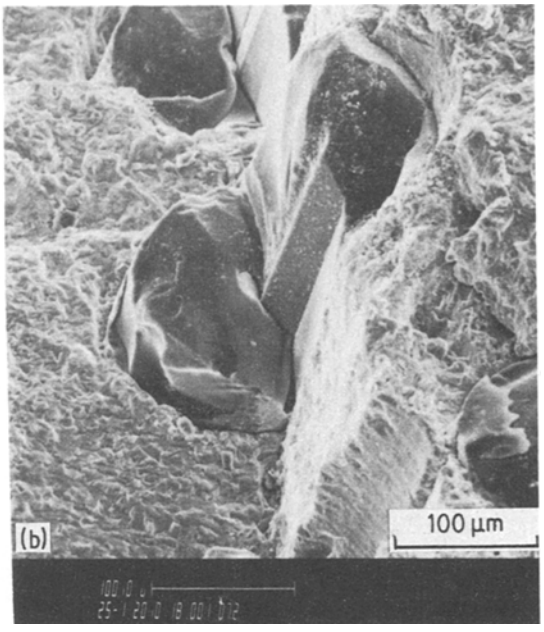

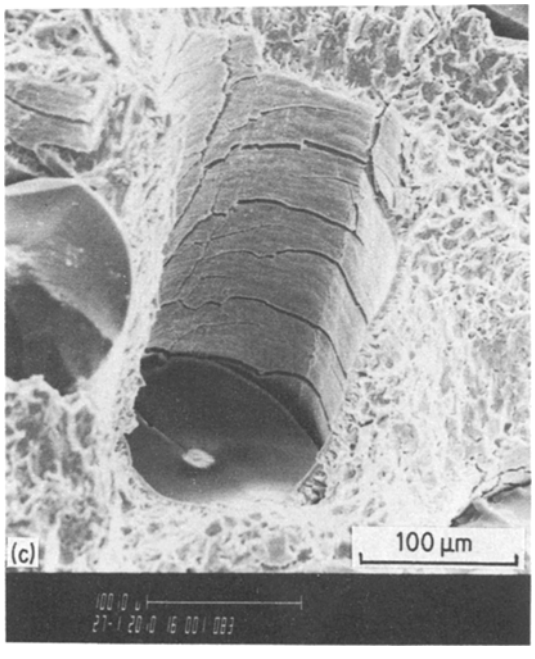

Figure 23 Scanning electron micrographs of failure surfaces according to sliding mode II: (a) Ti–6Al–4V matrix (isothermal exposure: 9 h, 850° C, (b) in boron fibre (isothermal exposure: 18 h, 850° C), (c) at fibre–matrix interface (isothermal exposure: 36 h, 850° C).

fracture occurs ahead of the apparent crack tip. The mechanisms which control these fractures are similar to the mechanisms described by Metcalfe [3] for static loading with respect to the reaction zone thickness:

(a) in as-fabricated composites boron filaments fail at thin intrinsic defects:

(b) for relatively thin reaction zones, filament failures initiate at cracks in boride reaction layers;

(c) for thick boride reaction layer thickness the reaction zone and the filaments crack simultaneously.

3. The remaining metallic ligaments between broken fibres give the material the potential for energy dissipation and fatigue according to the mechanisms well known for metals.

4. The effect of thermal exposure on crack growth and rupture mechanism can be described as follows:

(a) when the reaction zone thickness is very small, fibre breakage is due to the superposition of the stress concentration field ahead of the crack tip corresponding to the macrocrack and the stress concentrations corresponding to microdefects along the fibres: surface imperfections or microcracks in filament core (Fig. 27). For each fibre, the number of fractures depends on the extent of the stress concentration around the macrocrack tip. A low matrix yield strength leads to a large stress concentration area. On the other hand, an increase of the matrix yield strength by work hardening, leads to a reduction in the area concerned by the stress concentration. A low stress intensity factor gives rise to a large number of cycles and enhances the effect

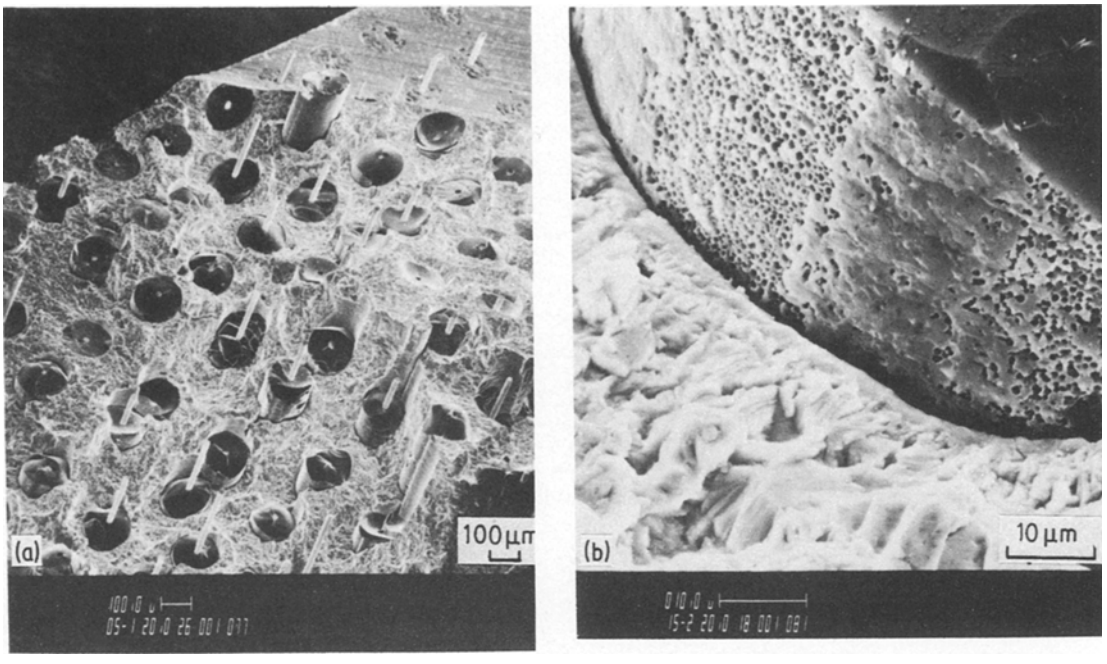

Figure 24 Scanning electron micrographs of failure surface showing filament degradation (isothermal exposure: 36 h, 850° C), (a) tungsten filament core pull-out, (b) boron filament surface porosity.

of cyclic work hardening on matrix ligaments necking around microcracks. Thus, the resulting effect of such a relatively low stress level is a smaller damaged zone. Otherwise, the relatively weak fibre–matrix bonding and the extensive plastic deformation of the matrix ligaments give rise to some debonding and a small pull-out effect (due to the tensile component of the stress field, perpendicular to the fibres);

(b) after relatively short isothermal exposure (e.g. 9 h at 850° C), the reaction zone is not thick

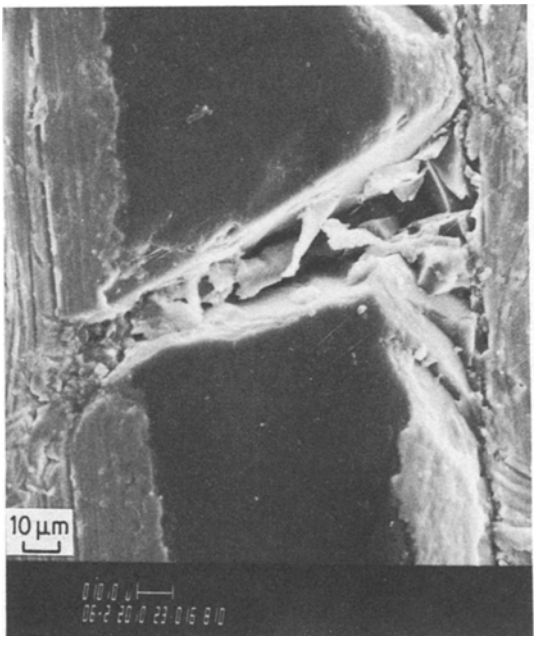

Figure 25 Scanning electron longitudinal micrograph of fibre crack growing into the matrix (isothermal exposure: 18 h, 850° C).

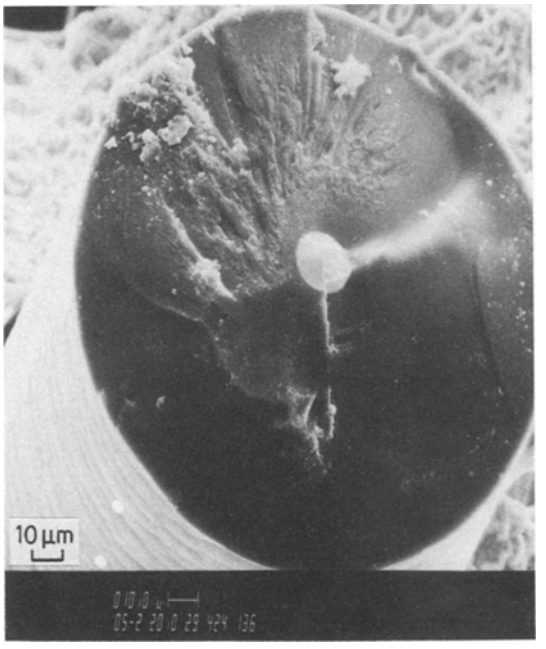

Figure 26 Scanning electron micrograph of boron filament fracture in as-fabricated B/Ti–6Al–4V composite.

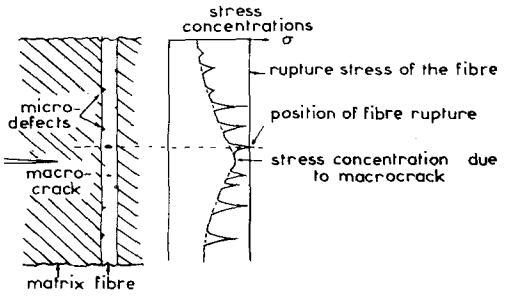

Figure 27 Distribution of the stress field along a fibre ahead of the macrocrack tip.

enough to degrade extensively the filament strength, but the fibre fractures are already initiated by microcracks in the reaction zone. Otherwise the interfacial bond is increased, rendering difficult any interfacial crack growth. The filaments are more effective in impeding the growth of transverse fatigue cracks because: (i) strong interfacial bonding prevents any pull-out phenomenon, (ii) the tensile component of the stress field perpendicular to the fibre ahead of the macrocrack tip increases, (iii) the triaxial state of stress causes plastic deformation of the matrix at a higher stress level according to failure criteria, (iv) microcracks propagate in the matrix from the fibre breaks, decreasing the stress concentration ahead of the main crack tip, (v) then the main crack has to join with the subcritical flaws by intermittent propagation in the fibre direction through longitudinal flaws in the filaments or local interfacial failure between fibre and reaction zone (Figs. 23 and 28).

The damage which occurs prior to propagation of the main crack in the area ahead of the crack tip is extended as a result of shorter critical load transfer length and better redistribution of elastic strain energy after the filament breaks. A decrease in interfacial failure improves the load transfer and allows the activation of microcracking occurring in the reaction zone along the filaments. This mechanism increases the number of fractures in each fibre and gives rise to a greater energy dissipation by matrix plastic deformation in a larger damage zone.

When the effect, previously described, of an isothermal exposure of relatively short duration seems to improve the composite vis à vis toughness, on the other hand, the absence of extended interfacial failure prevents the composite from becoming notch insensitive during fatigue loading at a low stress level.

Nevertheless, the occurrence of the damaging mechanism in the splitting zone, gives the material a pseudo-plastic behaviour in the vicinity of the cracks: the toughness is improved, the crack propagation rate and the exponent m decrease;

(c) the mechanisms of crack growth and rupture appear to be independent of reaction time, but the filaments are more and more degraded with time. Although the damage zone does not decrease in the related range of thermal exposure duration, the amount of plastic deformation in the matrix is less extensive because: (i) failures occur in the fibres at relatively low stresses, (ii) ductility of the matrix is reduced by a hardness increase. Hence the crack growth rate increase and the material behaves as a metal embrittled by the fibres and boron diffusion. The toughness decreases and m increases as for metals reinforced by brittle particulates [38].

Thus, the mechanisms of crack propagation and rupture are not the same for as-fabricated

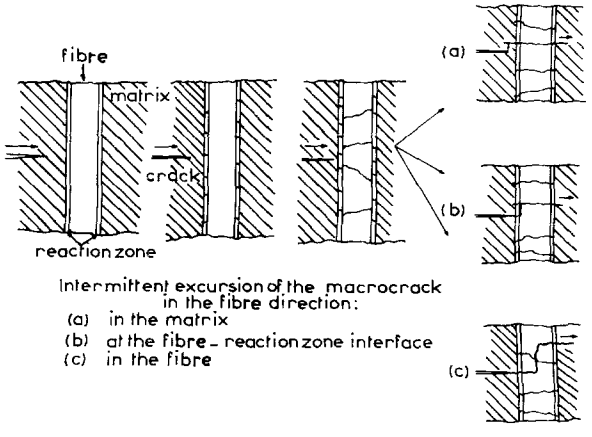

Figure 28 Damage mechanism initiated in the reaction zone when the macrocrack propagates.

and reacted composites. In the first case, crack propagation by fatigue and overloading is induced by fracture initiated in the fibre core and by interfacial failure causing some pull-out. In the second case, a damage mechanism initiated in the interfacial reaction zone leads to crack propagation in a zig zag manner though the main crack propagates macroscopically in a direction perpendicular to the reinforcement. In any case, fibre failure occurs ahead of the crack tip.

5.7. Rupture energy

Different energy dissipating mechanisms during composite failure have been proposed by several authors [39–52]. The principal contributions to the work of rupture deal with: fibre fracture, matrix failure, interfacial debonding, fibre pull-out, and redistribution of the elastic strain energy released after fibres break.

In order to explain the effect of isothermal exposure on the B/Ti–6Al–4V composites, the various contributions to the work of rupture have been assessed with the help of approximate formulae [41, 45, 46]. The numerical results reported in Table III suggest that the redistribution, from fibres to matrix, of the elastic strain energy released after fibres break and the energy corresponding to matrix failure, play a predominant role in determining the rupture energy.

Hence the non-monotonic change of the composite toughness with respect to thermal exposure can be explained by a simultaneous increase in the number of fibre fractures in the damage zone (resulting in energy redistribution increase) and a decrease of the fibre stress at composite rupture (decreasing the elastic strain energy release). This revolution is schematically illustrated in Fig. 29.

Since the elastic strain energy released after fibre fracture can be related to the change in the fibre strain at fracture compared with boride thickness, as reported by Metcalfe [3], an isothermal exposure of 9 h at 850° C is not an optimal heat treatment for better toughness. Indeed, after 9 h heat treatment, the reaction zone thickness is about 1 μm, which is already quite significant. Thus the duration of the heat treatment and even the temperature of the isothermal exposure have to be determined more precisely in order to provide that the interfacial failure makes way for the damage mechanism without excessively reducing the strength of the fibres.

6. Conclusions

Fatigue crack propagation testing is a suitable method to investigate simultaneously fatigue crack growth, overload crack propagation and rupture mechanisms in the case of metal matrix composites such as B/Ti–6Al–4V.

Although the accuracy of the results can obviously be improved (by using a more appropriate compliance function or a compliance calibration technique), these results are significant enough to represent the mechanisms of rupture and their evolution with isothermal exposure duration.

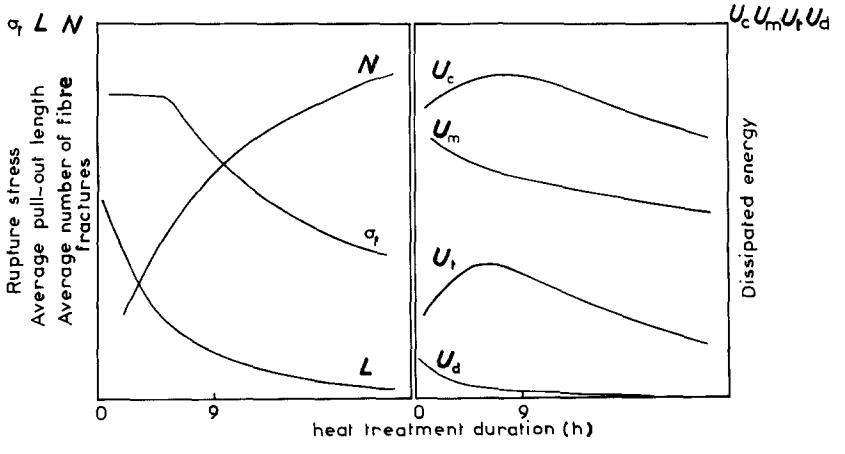

Figure 29 Schematic representation of the evolution of the failure work parameters plotted against isothermal exposure duration.

TABLE III Assessment of the contribution of the different energy-dissipating mechanisms, in B/Ti–6Al–4V composite

Energy dissipating mechanism	Fibre rupture energy, $U_f(J\,m^{-2})$	Matrix failure work,* $U_m(J\,m^{-2})$	Interfacial debonding energy, $U_d(J\,m^{-2})$	Fibre pull-out work, U_p	Elastic strain energy transferred from fibre to matrix, $U_t(J\,m^{-2})$	Total fracture work, $U_c(J\,m^{-2})$	
						derived from the different contributions	derived from the assessment of the toughness
Approximate Formula	$2\gamma_f V_f N$ (élastic strain)	$\frac{K_{ICm}^2}{E_m}(1 - V_f)$ (plastic strain)	$\frac{\sigma_f^2 L V_f}{2E_f}$ [52]	$\frac{\sigma_f L V_f}{12}$ [41]	$\frac{\sigma_f^2 L V_f N}{3E_f}$ [46, 49, 50, 52]	$U_f + U_m + U_d + U_t$	$\frac{K_{Iac}^2}{E_{eff}}$
For as-fabricated composite	≈ 30	≈ 30.000	≈ 1000	This energy is negligible since metallic ligaments are plastically shrunk before overall failure	≈ 2000	≈ 33000	≈ 32000
After isothermal exposure (9 h, 850° C)	≈ 100		≈ 0		≈ 6000	≈ 36000	≈ 37000

*The failure surface corresponding to intermittent excursion of crack in mode II has been considered neglibable with respect to failure surface normal to fibres.
$V_f = 0.32$; $E_f = 400$ GPa; σ_f(fibre stress at composite rupture): 3500 MPa (0 h); 3000 MPa (9 h).
$E_m = 108$ GPa; $K_{ICm} = 70\,MPa\,m^{1/2}$, γ_f(rupture energy of brittle boron filaments) $\approx 14\,J\,m^{-2}$.
E_{eff} = (effective Young's modulus of the composite) = 177 GPa derived from

$$1/E_{eff} = \left(\frac{1}{2E_T E_L}\right)^{1/2}\left[\left(\frac{E_T}{E_L}\right)^{1/2} - \nu_T + \frac{E_T}{2G_{LT}}\right]^{1/2}$$

N, average number of fractures for each fibre: 3(0 h); 12(9 h).
L, average distance between fibre microcracks in the vicinity of macrocrack: ≈ 0.2 mm ($L \approx l_c$).
K_{Iac}: $\approx 75\,MPa\,m^{1/2}$(0 h); $\approx 81\,MPa\,m^{1/2}$(9 h).

For as-fabricated composites, the mechanisms of rupture by fatigue and overload crack growth are controlled by intrinsic fibre defects, the fibre–matrix interfacial failure and the matrix ductility of the ligaments remaining between broken fibres.

A moderate heat treatment improves fibre–matrix bonding and, unexpectedly, increases toughness. This effect was explained by the build up of a damage mechanism initiated in the fibre–matrix reaction zone ahead of the macrocrack tip. The numerous fibre breaks occurring in a damage zone leads to energy dissipation by plastic deformation in the matrix.

After an isothermal exposure of long duration, the fibre strength is significantly lowered and at the same time the matrix ductility is diminished by boron diffusion. The composite becomes more and more brittle.

In as-fabricated composites, crack propagation is impeded by fibre–matrix delamination, rendering the composite notch-insensitive for low stress levels. After an isothermal exposure of short duration, the impeding effect of the fibre is still improved but caused by stronger interfacial bonding coupled with the damage mechanism. Intermittent crack growth according to mode II gives rise to the microscopic stepped appearance of the fracture surface and leads to irregularities in crack growth rate. Longer heat treatments decrease the impeding effect. Hence the composite behaves as titanium alloys embrittled by broken fibre particulates.

It is noteworthy that the mechanism leading to toughness increase is not related to a weakening of the interfacial bonding but rather corresponds to strong interfacial bonding associated with a damage mechanism.

Fatigue crack propagation testing is a useful technique for studying rupture mechanisms in these composites, because no important difference between fatigue crack growth and overload crack propagation mechanisms can be pointed out except that the overload zone exhibits ductile dimples at the fracture surface and large splitting zones, while the fatigue zone displays striations and a small damage zone.

Acknowledgements

The authors wish to thank Siemens Company for electrodischarged machining of the specimens.

References

1. K. G. KREIDER (ed.) in "Composite Materials", Vol. 4, Metal Matrix Composites (Academic, New York, 1974) Ch. 1, pp. 1–34.
2. A. G. METCALFE, *ibid.*, Ch. 6, pp. 269–327.
3. *Idem*, in "Composite Materials", Vol. 1, Interfaces in Metal Matrix Composites, edited by A. G. Metcalfe (Academic, New York, 1974) Ch. 3, pp. 65–123.
4. A. G. METCALFE and M. J. KLEIN, *ibid.*, Ch. 4, pp. 125–8.
5. R. NASLAIN, J. THEBAULT and R. PAILLER, Proceedings of the 1975 International Conference on Composite Materials (The Metallurgical Society of AIME, New York, 1975) pp. 116–36.
6. S. OCHIAI, and Y. MURAKAMI, *J. Mater. Sci.* **14** (1979) 831.
7. R. PAILLER, M. LAHAYE, J. THEBAULT and R. NASLAIN, in "Failure Modes in Composites IV", edited by J. A. Cornie and F. W. Crossman (The Metallurgical Society of AIME, New York, 1979) pp. 265–84.
8. M. Kh. SHORSHOROV, L. M. USTINOV, A. M. ZIRLIN, V. I. OLEFIRENKO and L. V. VINOGRADOV, *J. Mater. Sci.* **14** (1979) 1850.
9. S. OCHIAI and Y. MURAKAMI, *Met. Trans. A* **12A** (1981) 1155.
10. R. PAILLER, P. MARTINEAU, M. LAHAYE and R. NASLAIN, *Rev. Chimie Minérale* **18** (1981) 520.
11. M. Kh. SHORSHOROV, L. M. USTINOV, LE GUSKASJAN, L. V. VINOGRADOV and L. A. VERHOVSKI, *ibid.* **18** (1981) 427.
12. S. OCHIAI, K. OSAMURA and Y. MURAKAMI, "Progress in Science and Engineering of Composites", edited by T. Hayashi, K. Kawata and S. Umekawa, ICCM IV, Tokyo, (Okason and Co Ltd, Tokyo, Japan, 1982).
13. *Idem, Z. Metallkde* **74** (2) (1983) 68.
14. E. M. WU, in "Composite Materials", Vol. 5, Fracture and Fatigue, edited by L. J. Broutman (Academic, New York, 1974) Ch. 5, pp. 191–245.
15. J. R. HANCOCK, *ibid.*, Ch. 9, pp. 371–412.
16. K. M. PREWO, in "Composite Materials: Testing and Design (Third Conference)", ASTM STP 546 (American Society for Testing and Materials, Philadelphia, 1974) pp. 507–22.
17. W. R. HOOVER, *J. Compos. Mater.* **10** (1976) 106.
18. J. AWERBUCH and H. T. HAHN, *ibid.* **10** (1976) 231.
19. G. C. OLSEN and S. S. TOPKINS, in "Failure Modes in Composites IV", edited by J. A. Cornie and F. W. Crossman (Metallurgical Society of AIME, New York, 1977) pp. 1–21.
20. J. AWERBUCH and H. T. HAHN, *J. Compos. Mater.* **12** (1978) 222.
21. *Idem, ibid.* **13** (1979) 82.
22. G. J. DVORÁK and W. S. JOHNSON, *Int. J. Fracture* **16** (1980) 585.
23. R. T. BHATT and H. H. GRIMES, *Met. Trans. A* **13A** (1982) 1933.
24. A. SKINNER, M. J. KOCZAK and A. LAWLEY, *ibid.* **13A** (1982) 289.

25. G. JACOBSEN, "Progress in Science and Engineering of Composites", edited by T. Hayashi, K. Kawata and S. Umekawa, ICCM IV, Tokyo, 1982, pp. 1323.
26. H. ISHIKAWA and M. TAYA, *ibid.*, pp. 675.
27. M. J. OWEN and P. T. BISHOP, *J. Phys. D* **7** (1974) 1214.
28. A. W. HOULDSWORTH, S. MORRIS and M. J. OWEN, *ibid.* (1974) 2036.
29. M. K. WHITE and M. A. WRIGHT, *J. Mater. Sci.* **14** (1979) 653.
30. S. PARHIZGAR, L. W. ZACHARY and C. T. SUN, in "Fracture of Composite Materials", edited by G. C. Sih and W. P. Tamuzs, Proceeding of the second USA-USSR Symposium, (Martinus Nijhoff, The Hague, Boston, London, 1982) pp. 215-30.
31. S. V. HOA, A. D. NGO and T. S. SANKAR, *ibid.* pp. 477–84.
32. R. PAILLER, thesis, University of Bordeaux I, France (1979).
33. S. W. TSAI and H. T. HAHN in "Introduction to Composite Materials" (Technomic, Westport, Conneticut, USA, 1980).
34. R. J. NUISMER and J. M. WHITNEY, in "Fracture Mechanics of Composites", ASTM STP 593, (American Society for Testing and Materials, Philadelphia, 1975) p. 117.
35. S. W. TSAI and H. T. HAHN, in "Inelastic Behavior composite Materials", ASME AMD 13 (1975) p. 73.
36. E 647-78 T Annual Book of ASTM Standards, May (1978).
37. D. W. HOEPPNER and W. E. KRUPP, *Eng. Fract. Mech.* **6** (1974) 47.
38. L. P. POOK and R. A. SMITH, "Fracture Mechanics", edited by R. A. Smith (1979) pp. 29-67.
39. A. KELLY, *Proc. R. Soc.* **A282** (1964) 63.
40. J. COOK and J. E. GORDON, *ibid.* **A282** (1964) 508.
41. A. KELLY, in "Strong Solids" (Oxford University Press, 1966).
42. C. GURNEY and J. HUNT, *Proc. R. Soc.* **A209** (1967) 508.
43. G. A. COOPER and A. KELLY, *J. Mech. Phys. Solids* **15** (1967) 279.
44. *Idem*, in "Interfaces in Composites", ASTM, STP 452 (American Society for Testing and Materials Philadelphia, 1969) p. 90.
45. J. O. OUTWATER and M. C. MURPHY, 24th Annual Technical Conference, Society of Plastic Industry Section 11-C, (1969) p. 1.
46. M. PIGOTT, *J. Mater. Sci.* **5** (1970) 669.
47. J. AVESTON, G. A. COOPER and A. KELLY, Proceedings NPL Conference on "The Properties of fibre composites", (IPC, London, 1971) p. 15.
48. B. HARRIS, P. W. R. BEAUMONT and E. MONCUNILL DE FERRAN, *J. Mater. Sci.* **6** (1971) 238.
49. P. W. R. BEAUMONT, J. FITZ-RANDOLPH, D. C. PHILIPS and A. S. TETELMAN, *J. Compos. Mater.* **5** (1971) 542.
50. *Idem, ibid.* **7** (1972) 289.
51. P. W. R. BEAUMONT and B. HARRIS, *J. Mater. Sci.* **7** (1972) 1265.
52. T. U. MARSTON, A. G. ATKINS and D. K. FELBECK, *ibid.* **9** (1974) 477.

Received 28 December 1984
and accepted 31 January 1985